Cryogenic detectors for particle physics

L. Gonzales-Mestres, D. Perret-Gallix

CRYOGENIC DETECTORS FOR PARTICLE PHYSICS

L. Gonzalez-Mestres and D. Perret-Gallix

LAPP, B.P. 909, F-74019 Annecy-le-vieux Cedex, France

Abstract: A comprehensive introduction to cryogenic detector developments for particle physics is presented, covering conventional detectors cooled to low temperature (scintillators and semiconductors), superconductive and thermal sensitive devices, as well as the basics of cold electronics. After giving a critical overview of current work, we elaborate on possible new ways for further improvements and briefly evaluate the feasibility of the main proposed applications.

Résumé: Ce cours est une introduction générale aux développements récents sur les détecteurs cryogéniques pour la physique des particules. Il décrit les propriétés à basse température des détecteurs conventionnels (scintillateurs, semiconducteurs), ainsi que les systèmes supraconducteurs, les détecteurs thermiques et l'électronique refroidie. La présentation du panorama des travaux en cours est complétée par une discussion des améliorations possibles ainsi que par une brève évaluation de la faisabilité des expériences proposées.

1. INTRODUCTION

Several fashionable subjects in particle physics require high sensitivity detectors, dedicated to high precision measurement of low energy particles. Among the relevant physics issues are: electron neutrino mass [1], double β decays [2], solar neutrinos [3], cosmic, solar or laboratory-produced axions [4], galactic dark matter [5], cosmological neutrinos [6],... There may also exist weakly ionizing particles, such as magnetic monopoles [7], that would be difficult to detect by conventional techniques.

The growing prominence of this "new" physics in the context of contemporary science has triggered specific detector developments, aiming to satisfy the requirements of a particular experiment: small bolometers [8] or superconducting tunneling junctions (STJ) [9] to measure the mass of the electron neutrino; superheated superconducting granules (SSG) [10, 11, 12] and STJ [13] for solar neutrino detection; large bolometers [14, 15] for double β experiments; low temperature electromagnetic cavities [16, 17] for cosmic axions; SSG [18, 19], bolometers [14, 20] or ballistic phonon devices [21, 22] for dark matter searches; induction loops [21, 23] or SSG [24] for magnetic monopoles... All these techniques are based on the following properties of matter at low temperature:

a) Lower excitation energies. A single ballistic phonon has $E < \hbar\omega$ (Debye) < 0.1 eV, and is able to excite one or several quasiparticles in superconductors. In ordinary superconductors, the energy gap Δ for quasiparticle excitation lies in the range 10^{-6}-10^{-3} eV [26], whereas high T_c materials ($T_c \simeq 100$ K) [25] have $\Delta \simeq 2 \times 10^{-2}$ eV. Thermal phonons have $E \simeq kT \simeq 10^{-5}$ eV at 0.1 K. Spin systems involving Kramers doublets can also produce excitation energies as low as 10^{-6} eV [15]. This is to be compared to the intrinsic semiconductor energy gap (≈ 1 eV), or to the energy of visible photons produced in scintillators (≈ 3 eV).

With elementary excitations in the range 10^{-6}-10^{-5} eV, the energy dependent statistical component of energy resolution becomes very small. Optimal energy resolution is then mainly given by the read-out noise and thermal fluctuations of the detector.

b) The fast decrease of specific heats for dielectric crystals and semiconductors:

$$c \text{ (lattice)} \simeq a\,(T/\Theta_D)^3 \qquad \{1a\}$$

$$c \text{ (superconducting electrons)} \simeq c \exp(-\Delta/kT) \qquad \{1b\}$$

where $a \simeq 234\ n\ k$ (n = ion density) and Θ_D is the Debye temperature. Expression (1a) is actually not an exact one, and in practice a T-dependent Θ_D must be used. More detailed expressions for (1b) can be found in [26]. This sharp fall of specific heat at very low temperature makes possible thermal detection, where a small increase in temperature can be detected with the help of special thermometers. Normal electrons are less favored, since their heat capacity decreases only linearly with T.

c) At low temperature, thermal noise decreases for both detector and electronics. This may be crucial for the detection of very small signals and often determines the sensitivity threshold.

d) Low temperature phenomena provide specific signals (e.g. change in magnetization) or amplification effects (e.g. metastable phase transition in superconductors, latent heat release or quasiparticle multiplication). These effects can be the basic principle of some devices, or may provide a way to enhance the sensitivity of other detectors. Furthermore, a wide variety of superconductive materials and crystal heat absorbers is available and can be used as dedicated active targets. Then, a low temperature detector may prove useful even if its intrinsic performance is no better than that of NaI(Tℓ) or ultrapure germanium.

However, several difficulties specific of cryogenic devices have to be solved before taking benefit of these features:

a) At very low temperature, relaxation processes are rather slow (e.g. quasi-particle or spin-lattice relaxation, electron-hole recombination, ballistic phonon thermalization, heat or radiation release by metastable states,...). Furthermore, electrons ($v \sim 10^6$ cm s^{-1}), ballistic phonons ($v \sim 4\ 10^5$ cm s^{-1}), and, a fortiori, heat propagate much slowlier than light. This makes difficult to reach time resolution below several microseconds and in some cases rise times longer than 1 msec are reported. Nevertheless, the superconducting to normal phase transition has a very fast intrinsic time scale (10^{-12} s for elementary Cooper pair breaking) and luminescence still exists at very low temperature, as will be discussed later on.

b) To reach optimal performances, a considerable technological effort is required: temperature gradients may spoil uniformity in detector response; fluctuations in the mechanisms of energy conversion contribute to the energy resolution; Kapitza resistances must be kept as low as possible in order not to slower detector response; energy lost in irreversible mechanisms (e.g. Frenkel pairs created by α particles) must be taken into account, as well as energy trapping by long-lived electronic states (e.g. impurity levels); luminescence phenomena, if out of control, will further degrade energy resolution... All these problems are being dealt with in current developments.

c) Besides the eventual inconvenience of lengthy cooling and reheating procedures (particularly for large detector at very low temperature), cryogenic devices must exhibit good stability over thermal cycles.

Fig. 1 shows the T-dependence of the effective Θ_D for several semiconductors, whereas Fig. 2 exhibits the specific heat anomaly from electrons in a conventional superconductive material. Specific heats of high T_c superconductors are currently being studied. As an example, YBaCuO specific heat is exhibited in Fig. 3. The appearance of a peculiar "low T" term seems to be a common feature to several high T_c materials. Fig. 4 shows the thermal conductivity of a metal in both superconducting and normal phase, where the electron anomaly at $T < T_c$ reflects the fact that Cooper pairs are not entropy carriers. Heat propagation at quasi-equilibrium is governed by the coefficient $D = \kappa/c$, according to the usual diffusion equation, but for pure high quality crystals the concept of ballistic phonons plays a fundamental role. At very low temperature, the intrinsic lattice thermal conductivity is limited only by umklapp processes (where momentum is conserved up to a reciprocal lattice vector) [27], and increases exponentially in Θ_D/T. Then, the effective thermal conductivity is controlled by surface scattering, impurities and defects. Its T-dependence follows that of specific heat (T^3 law). For a perfect, infinite ionic crystal at $T = 0$, one would have $D = \infty$ and phonons would propagate ballistically at the speed of sound. Fig. 5 shows the T-dependence of κ for several isotopically pure LiF crystals of different sizes [28]. Below $T = 10$ K, the measured thermal conductivity is proportional to the crystal size, which provides evidence for linear (non-diffusive) propagation of unscattered phonons through the crystal.

An important question is the microscopic description of the energy degradation of an ionizing particle or a recoiling nucleus in the detector. A ionizing particle in a superconductor first produces excited electrons, which interact with other electrons and radiate phonons. Such phonons break Copper pairs. After several levels of energy degradation ($\sim 10^{-10}$ s), an excess of $\sim 10^9$ quasiparticles per MeV has been produced. A detailed description can be found in [29]. Nucleus recoil has been studied in [30]. Further studies are required for each specific medium, to better understand the detector response as well as effects spoiling energy resolution.

The field of low temperature detectors for particle physics is a recent one, still at the stage of feasibility studies. However, in the last two years, encouraging results have emerged [31, 32, 33] as the development effort increases. Interesting new ideas have also been put forward, but there is still room for further innovation.

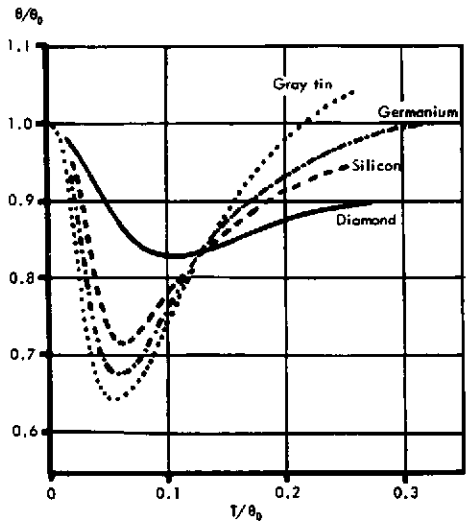

Fig. 1: T-dependence of the effective Debye temperature for several semiconductors. Diamond, silicium and germanium are often used as bolometers at very low T. From: E. Gopal, "Specific Heats at Low Temperature", Ed. Heywood 1966.

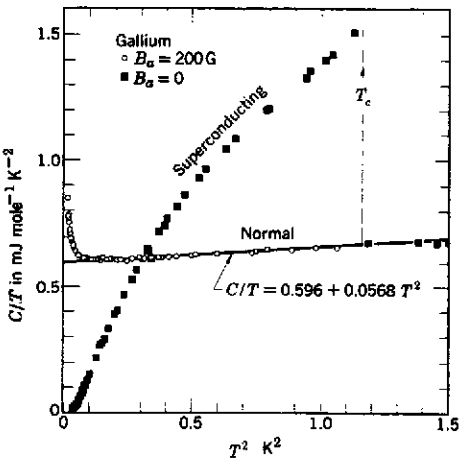

Fig. 2: Specific heat of gallium in both normal and superconducting phase. The linear T-dependence of normal electron heat capacity is to be compared to the exponential behavior of c (electrons) in the superconducting phase. From: C. Kittel, "Introduction to Solid State Physics", Ed. Wiley 1968.

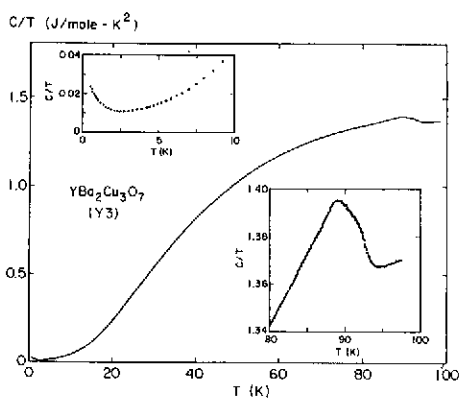

Fig. 3: Detail of the specific heat of a "high T_c" superconductor. From: R.A. Fischer, J.E. Gordon and N.E. Phillips, LBL preprint (1988).

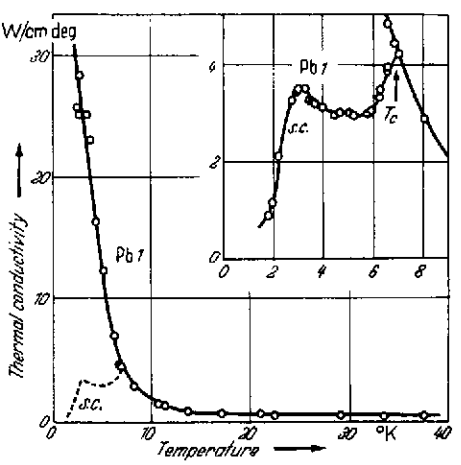

Fig. 4: Thermal conductivity of lead in both normal and superconducting phase. From: Handuch der Physik, Ed. Springer-Verlag.

2. CONVENTIONAL DETECTORS AT LOW TEMPERATURE

2.1 Scintillators

Luminescence is not specifically a room temperature phenomenon. If a high light yield is the main requirement, together with the use of a specific target, thermal quenching [34, 35] may enforce the use of cryogenics. Several well known scintillators exhibit a higher light yield at low temperature, although such an improvement is accompanied by an increase of fluorescence decay time. Naively,

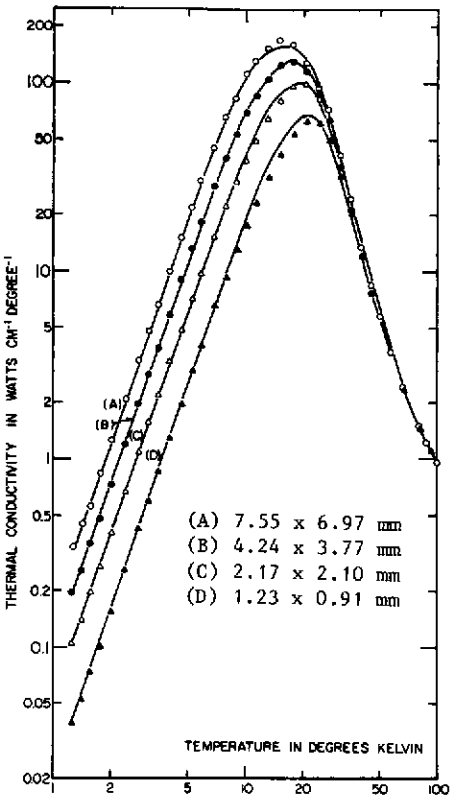

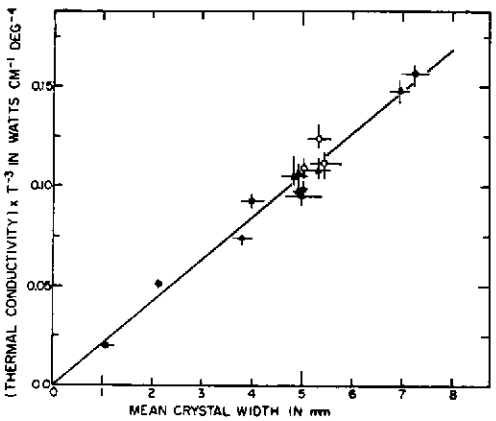

Fig. 5: Measured thermal conductivity of pure LiF crystals at low temperature.
Left: T-dependence of κ for several crystal sizes.
Above: size-dependence of the coefficient of the T^3 term at $T < 10$ K.

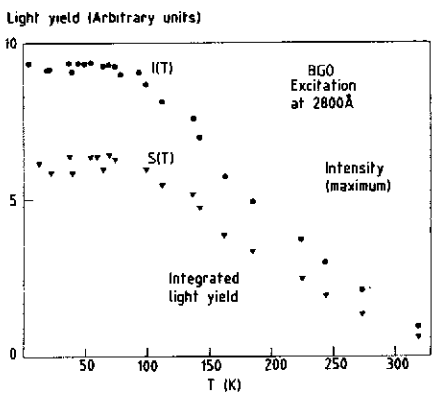

Fig. 6 (above): T-dependence of BGO light yield. From [37].

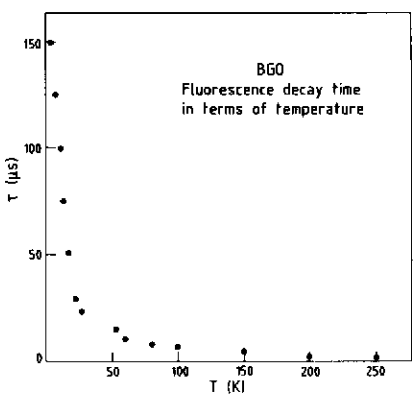

Fig. 7 (left): T-dependence of BGO fluorescence decay time. From [37].

one has [34]:

$$1/\tau = p_r + p_{nr} \qquad (2)$$

where τ is the decay time, p_r the probability for radiative transitions and p_{nr} the probability of non-radiative de-excitation due to orbital band crossing [35]. As T decreases, each electron tends to remain in the lower level of its orbital band, and only radiative processes are allowed. This leads to the law:

$$\tau(T)/\tau(0) = \eta(T)/\eta(0) \qquad (3)$$

where η is the fluorescence efficiency. However, expression (3) ignores exciton trapping by metastable states [36], originating from low lying vibrational modes (self-trapping), or from impurity levels

slightly below the usual band. Let $\Delta\varepsilon$ be the energy difference between the fluorescent perturbed level and the metastable state (e.g. the lowest vibrational state of the band), and p_r' the decay time of the metastable level. At low T [37]:

$$1/\tau \simeq (p_r' + p_r\, e^{-\Delta\varepsilon/kT})\,(1 + e^{-\Delta\varepsilon/kT})^{-1} \qquad \{4a\}$$

so that, for $kT \ll \Delta\varepsilon$, one has: $\tau^{-1} \simeq p_r'$. According to this description, the decay time tends to a constant at $T \to 0$, but its value can be significantly larger than that predicted by equation {3}. Exciton trapping appears to be present in several well known scintillators, whose light yield increases or remains unchanged when going down in T. BGO light yield increases by a factor of 10 between T = 300 K and T = 4 K, whereas the decay time varies from 300 ns to 150 μs. A fit to low temperature decay time for BGO and Bi^{3+} doped luminophores suggests a law similar to {4a}:

$$\tau \simeq (A + B\, e^{-\Delta\varepsilon/kT})^{-1} \qquad \{4b\}$$

with the values [37, 36]:

Crystal	A (s^{-1})	B (s^{-1})	$\Delta\varepsilon$ (meV)
$Bi_4Ge_3O_{12}$	$5\ 10^3$	$1.3\ 10^5$	2.85
$LaPO_4$(Bi) 1%	$0.6\ 10^3$	$3.05\ 10^5$	2.09
YVO_4(Bi) 1%	$6\ 10^3$	$2.65\ 10^5$	1.03
$CaWO_4$	$5.2\ 10^3$	$6.0\ 10^4$	4.5

Fig. 6 exhibits the T-dependence of BGO light yield, whereas Fig. 7 shows the T-dependence of fluorescence lifetime. BGO transparency has also been found to improve at low temperatures [38]. For $CaWO_4$ [36], the light yield remains unchanged whereas τ increases from 20 μs at room temperature to 200 μs at T = 4 K. Recent measurements [39] with a well known tungstate scintillator, $CdWO_4$, show a similar behavior down to 1.5 K. Rise times have not been measured in detail, but are expected to be considerably faster.

Even more interesting may be Ce^{3+} doped compounds. The fluorescence of YAG:Ce (a laser material [40]) was reported to decay in 16 nsec at room temperature [41], and in 60 ns at T = 4.4 K [42]. Detailed studies of Ce-doped crystals at low temperature are needed, including the commercially available GSO:Ce (Gd_2SiO_5 doped with Ce^{3+} [43]).

If a fast cryogenic scintillator sensitive to low energy particles can indeed be found, it may be possible to combine luminescence (giving fast timing) with thermal detection (giving energy resolution). This possibility will be dealt with in chapter 3. However, luminescence studies at very low temperature are far from being systematic, and very little information exists below 1 K. A full research program down to 100 mK or even lower T is required, in order to really evaluate the potentialities of scintillators as cryogenic detectors.

2.2 Semiconductor detectors.

Semiconductor detectors at room temperature exhibit already rather satisfying figures. Junction detectors of a few mm^2 have provided for decades $\approx$ 15 keV energy resolution (including thermal noise) on 5.47 MeV ^{241}Am α's. More recently, larger detectors have been developed and they are often cooled to LN_2 temperature. A basic parameter characterizing the behavior of semiconductors is the number of carriers. In a pure intrinsic semiconductor (Si, Ge...), $n = p = n_i$ (intrinsic carrier density). n_i is given by the expression [44]:

$$n_i = 4.9 \times 10^{15}\,(m_{dh}\, m_{de} / m_o^2)^{3/4}\, M_c^{1/2}\, T^{3/2} \exp(-\varepsilon_g/2kT) \qquad \{5\}$$

where ε_g is the gap energy, M_c the number of equivalent minima in the conduction band, m_{dh} and m_{de} the "density of state" effective mass for holes and electrons, and m_o the electron mass. A second basic parameter is the mobility μ, defined through the relation:

$$v_d = \mu\, E_{el} \qquad \{6\}$$

where v_d is the drift velocity of carriers in the presence of an electric field E_{el}. The mobility in the presence of acoustic phonons varies as:

$$\mu_\ell \sim (m^*)^{-5/2}\, T^{-3/2} \qquad \{7\}$$

where m^* is the carrier effective mass. Scattering with phonons can thus be suppressed by lowering the temperature. In intrinsic semiconductors, however, at very low T, the conductivity $\sigma = n\mu_n + p\mu_p$ is strongly damped by the fall in carrier population. Intrinsic semiconductor detectors (e.g. ultrapure germanium) are based on the excitation of a certain number of electrons from the valence band to the conduction band. This is a non-equilibrium process, where the signal must be collected before relaxation restores thermodynamical equilibrium. At low temperature, the population of quasiparticles decreases like $\exp(-\varepsilon_g/kT)$, whereas the phonon population varies as usual like T^3. In the absence of trapping energy levels, recombination is also damped by a factor $\exp(-\varepsilon_g/kT)$. The interest of low temperatures is limited by: a) the intrinsic energy resolution, depending on the energy deposition and the semiconductor energy gap; b) carrier trapping by frozen impurities. Even if the carrier mean free path is very long and the electronic noise is set very low, the statistical energy resolution will be given by:

$$\Delta E \simeq (f\, E\, \varepsilon)^{1/2} \tag{8}$$

where E is the deposited energy, ε the effective carrier excitation energy and f the Fano factor [45], related to the amount of energy transmitted to phonons. Typical values of f are 0.13 for Ge and 0.15 for Si. Germanium ($\varepsilon_g = 0.7$ eV) is operated at LN_2 temperatures giving $\approx 0.1\%$ energy resolution for ^{76}Ge double β experiments (Q = 2.04 MeV) [46], whereas InSb [47] ($\varepsilon_g = 0.23$ eV) is operated down to 1.5 K for the detection of infrared photons. InSb is also favored because of its very high mobility (8×10^4 cm^2 V^{-1} s^{-1} at room temperature).

Extrinsic semiconductors have the advantage of being able to produce extremely low values of the energy gap. Some examples are: 0.0093 eV for Ge:Li (donor); 0.033 for Si:Li (donor); 0.045 for Si:B (acceptor) ; 0.0058 for GaAs:Si (donor). Doped semiconductors allow to obtain excellent figures in energy resolution for low energy particles (e.g 150 eV FWHM energy resolution for Si:Li irradiated with 6 keV γ's at LN_2 temperatures). However, because of doping impurities, it becomes more difficult to extract the carriers from a bulk sample. Neglecting phonon scattering, mobility in the presence of ionized impurities follows the law:

$$\mu_i \sim (m^*)^{-1/2}\, N_i^{-1}\, T^{3/2} \tag{9}$$

where N_i is the ionized impurity density. On the other hand, at higher temperatures acoustic phonon scattering becomes important. Thus, mobility is limited at low temperature by the dopant concentration or just the intrinsic impurity concentration, and at room temperature by thermal phonons. The main problem is therefore to optimize doping (or purity) and operating temperature. High resistivity is required to apply a high E_{el} without creating a large leakage current. But mobility must remain high, and carrier lifetime must be long enough. If the drift velocity and detector size are such that carriers cannot reach the electrodes in a time much shorter than their lifetime, important losses will appear and the detector performance will be degraded. This is the main difficulty to build large detectors with extrinsic semiconductors, and has led to the development of dedicated technologies [48].

Fig. 8 shows the carrier density of intrinsic Si as a function of temperature, whereas Fig. 9 exhibits the mobility of several semiconductors as a function of T for several impurity concentrations.

3. BOLOMETERS

In an insulating crystal at low temperature, an energy deposition E will lead to an increase in temperature that can be detected with a resistive thermometer (thermistor). Neglecting read-out noise and assuming that the deposited energy have been fully converted into heat, energy resolution is given by phonon thermal fluctuations [49]:

$$\Delta E_{rms} \simeq \zeta\, (C/k)^{1/2}\, kT \propto T^{5/2} M^{1/2} \tag{10}$$

where C is the heat capacity, k the Boltzmann constant and M the mass of the crystal. The heat capacity of the thermistor has been neglected, which may not be correct for small bolometers. The coefficient ζ depends on the details of detector architecture, but is often estimated to be in the range 1.5-2. Thus, a sizeable increase in detector mass can be compensated by a moderate decrease in temperature.

In practice, a considerable technological effort is required before reaching such an ideal scenario: some energy is trapped by impurities in long lived metastable states; scintillation light is also produced and may escape the detector; the thermistor specific heat does not follow a T^3 law and its heat capacity may dominate the detector one at very low T; heavily ionizing particles (e.g. α's) lose, also, energy in creating Frenkel pairs of dislocations... Finally, the development of linear low noise amplifiers for bolometric read-out is far from being a trivial problem.

The measurement of the ν_e mass from the ^{3}H Kurie plot can be made with detectors smaller than 1 mm^3. Energy resolution of 10 eV FWHM or less on 18.6 keV electrons is needed for such purposes.

A diamond bolometer (0.25 mm^3) at 1.3 K reached FWHM energy resolution of 36 keV on 5.5 MeV α particles [8], and at 100 mK a composite Si micro-calorimeter brought 17 eV FWHM resolution on 6 keV γ's [50]. Fig. 10 shows the scheme of the Wisconsin-Goddard Si bolometer, whereas Fig. 11 exhibits spectra obtained with this device.

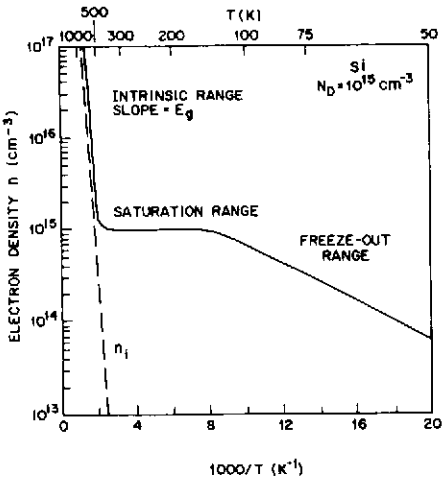

Fig. 8: Density of carriers for intrinsic silicium versus T. From [44]. Carrier population drops for T below T≃ 120 K, due to the Boltzmann factor.

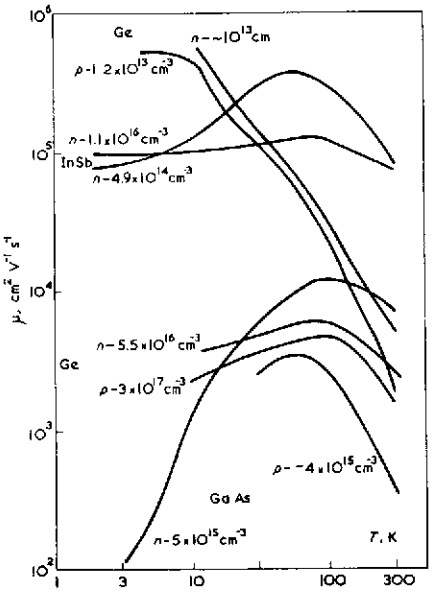

Fig. 9: T-dependence of carrier mobility for doped Ge, GaAs and InSb. From: B. Lengeler, Cryogenics 14, 439 (1974). Doped Ge and InSb exhibit particularly good low T behavior.

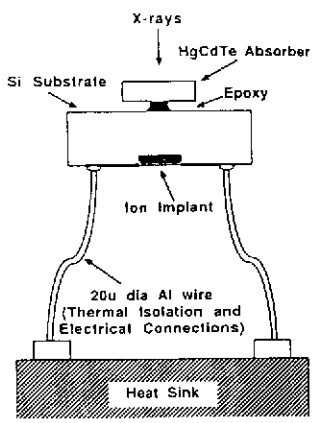

Fig. 10: The Si micro-calorimeter described in [50]. The ion implant is the main ingredient of the thermal sensor.

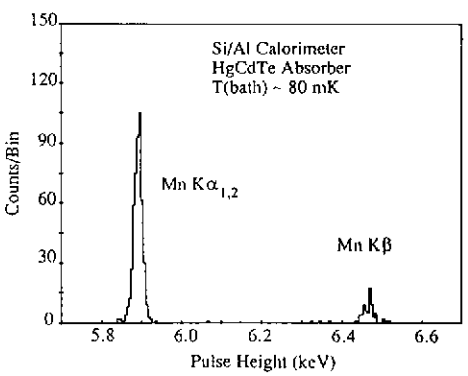

Fig. 11: Low energy γ spectra from [50], indicating ΔE (FWHM) $\simeq$ 17 eV from the width of the Mn K_α peak.

More recently, the study of large bolometers has also been undertaken. Using a 0.7 g germanium absorber at 44 mK, the Milano group [51] obtained 1% energy resolution on α particles from a ^{228}Ra source in radioactive equilibrium with its daughters. Furthermore, a previous high flux irradiation allowed to implant daughter nuclei in the crystal producing satellite peaks shifted upwards by 100 keV (Fig. 12a). As the implanted nuclei decayed, the satellite peaks disappeared and only single peaks from external α's remained (Fig. 12b). The authors conclude that the bolometer was sensitive to nucleus recoil, as expected from the 50 keV energy resolution. Similar evidence had been previously reported from work with small bolometers [52].

A new idea is the so-called "magnetic bolometer" [15]. About half of the deposited heat is converted into very low energy spin excitations ($\sim 10^{-6}$ eV) of a Kramers doublet. A small change in the magnetization of the crystal can then be detected by a SQUID read-out. The authors report 30 keV equivalent noise at 400 mK with 5.5 MeV α's on a 7.35 g sapphire absorber with a 135 mg YAG:Eb^{3+} magnetic bolometer implanted on the sapphire. However, because of the above mentioned energy trapping by excitons, Frenkel pairs, and other effects, a direct check of energy resolution is required before evaluating the real performance of the detector.

In some applications, time resolution may be important for event identification and background rejection. Large bolometers are not fast detectors. The Milano bolometer gives rise times of the order of 200 μs and the one from [15] exhibits a 200 ms rise time. Perhaps bolometry should in some cases be combined with other detection techniques (luminescence?) in order to produce a primary fast signal as timing strobe. If light is used as a complementary signature, particle identification can be achieved through the heat-light ratio, where, for a given energy, nucleus recoil is expected to be less luminescent than ionizing particles. Although much more work on the subject is needed, the idea of combining thermal and photosensitive read-out in a single device would in principle allow to detect all the deposited energy, contrary to present scintillators. Some well-known luminophores (silicates, germanates, aluminates,...) have reasonably high Debye temperatures and would be well suited for this purpose. Ultrapure intrinsic semiconductors may eventually lead to composite-read-out devices, where besides the usual electrodes for carrier detection, a thermometer would measure the energy converted into heat. Again, particle identification would be achieved through the current/heat ratio.

Another point requiring careful study is the possible use of a superconducting absorber as the specific target (e.g. ^{100}Mo for double β experiments). Quasiparticle lifetime is then a crucial parameter to estimate the detector response. Fig. 13 shows the result of a theoretical calculation of τ_r (recombination time) and τ_s (thermalization time, associated to phonon scattering). It may often happen that, at low reduced temperature ($t = T/T_c$), quasiparticles have rather long lifetimes and reach ballistically the detector walls. In such case, one may attempt to collect them with electrodes implanted on the detector surface, while a thermometer measures the thermalized signal. A more orthodox alternative would be to incorporate such target elements in high Θ_D oxides, but it is not obvious that the purity level required for low background experiments can still be preserved.

To date, the main motivation for the development of large bolometers (100 g - 1 Kg) lies in neutrinoless double β decays [14], where energy resolution is crucial for background rejection, and dark matter searches through nucleus recoil [53], where sensitivity to energy deposition below 1 keV is required. More difficult, because of background, would be a solar neutrino experiment based on ν-e^- scattering using several tons of bolometric detector [20]. Applications at reactors would have to face similar problems.

4. SUPERCONDUCTING TUNNELING JUNCTIONS

Superconductors provide the unique possibility of producing diodes with about 10^{-3} eV current carrier excitation energy. Then, a statistical $N^{1/2}$ law (Poisson distribution) for energy resolution leads again to exceptional performances for the detection of low energy particles. In a STJ with a small bias voltage, quasiparticles and holes excited by incident radiation tunnel across a thin insulating layer separating two superconducting samples, and the current can be read with conventional low noise pre-amplifiers.

Usually, STJ are made of two metallic films separated by the insulating layer. A typical design can be seen in Fig. 14. STJ are not expected to be massive detectors, but new ideas have recently emerged (e.g. quasiparticle trapping, which also provides multiplication [13]) to incorporate bulk superconducting specimens.

The bias voltage creates a thermal current $I_{th} \propto \exp(-\Delta/kT)$ that can be lowered by working at low reduced temperature. In order to prevent Cooper pair tunneling (DC-Josephson current), a magnetic field parallel to the oxide barrier is applied. An incoming particle will excite mainly electrons of energy much larger than the gap Δ, but these electrons will later relax emitting phonons. At $t \ll 1$, phonons mainly excite quasiparticles, which can then tunnel across the junction or recombine. The expected energy resolution in a STJ follows the same expression as for the semiconductor, given by (8). Potentially, a Sn-SnO-Sn detector with $f \simeq 1$ and $\varepsilon \simeq \Delta \simeq 0.6$ meV, should reach 0.1% energy

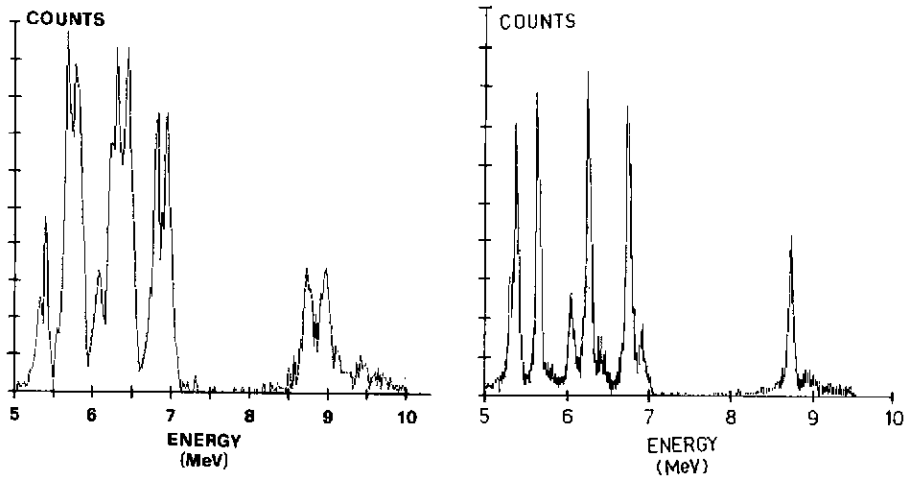

Fig. 12: Energy spectra of the Milano bolometer exposed to a ^{228}Ra source: a) with daughter nuclei inside the crystal; b) after the decay of implanted daughter nuclei.

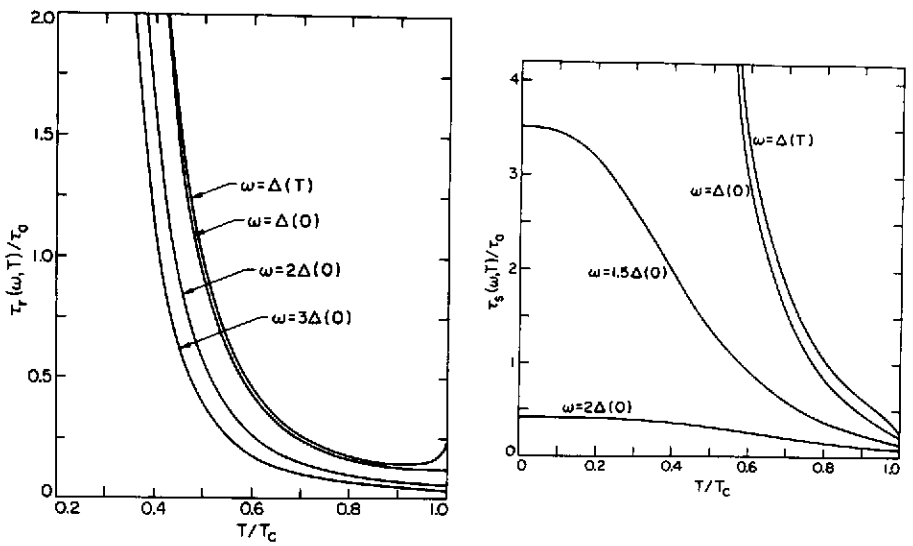

Fig. 13: Quasiparticle recombination time (left) and quasiparticle-lattice relaxation time (right), in terms of T and the quasiparticle energy ω. From: S.B. Kaplan et al., Phys. Rev. B14, 4854 (1976). τ_0 depends on the material used, but is larger for harder metals: 7.5 10^{-11}s for Hg, 2.3 10^{-9} s for Sn, 4.4 10^{-7} s for Al.

resolution on 6 keV γ's. Experimental results are not that good, but the SIN group claims [54] 48 eV FWHM resolution based on the width of the 5.89 keV ^{55}Mn K_α peak (Fig. 15), obtained with a Sn STJ operating at $T \simeq 400$ mK. The Garching (TMU) group in turn reports [55] 88 eV resolution, determined from the energy difference between the K_β (6.49 keV) and K_α peaks (Fig. 16). A typical signal rise time from existing STJ is of the order of 15 μs.

Using materials with higher T_c, a low value of t can be reached at ^{4}He temperatures. An excellent result has recently been provided by a 10 μm × 10 μm Nb/Al/Al_2O_3/Al/Nb junction [56], reaching a 250 eV energy resolution for 6 keV γ's at T = 1 K. If electronic noise can be lowered, the optimal energy resolution given by Poisson's law has been estimated to: ΔE (FWHM)$\simeq$10 eV. Nb based junctions present the advantage of a better thermal stability and device life time. Although rather small with present technology, such junctions can be used for astrophysical purposes.

Apart from the detection of low energy γ rays, a possible use of small STJ would be neutrino mass measurements [9], but if larger devices can be made, they could be used [13] to detect low energy solar neutrinos through the ^{115}In Raghavan's reaction [57]. A ^{115}In detector may also be used for $\bar{\nu}_e \rightarrow \nu$ oscillation experiments at reactors.

STJ provide an interesting read-out for crystal phonon detectors, where ballistic phonons would be converted into quasiparticles. Since ballistic phonons propagate along the main crystallographic axis, it should be possible to extract information on the position of the event inside the crystal [21, 22]. This possibility has been recently demonstrated by the Garching (TMU) group [22] using three aluminum STJ implanted on one of the faces of a Si wafer, and moving the incident position of α particles on the other side of the crystal (Fig. 17a). Position information is seen to emerge from correlations between the signals observed at two different junctions (Fig. 17b). A parallel effort along similar lines is being pursued by the Stanford group [21].

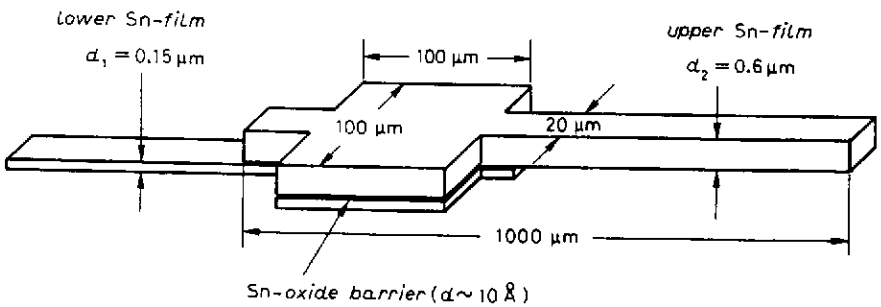

Fig. 14: A schema of STJ prepared at PSI (Villigen) [54].

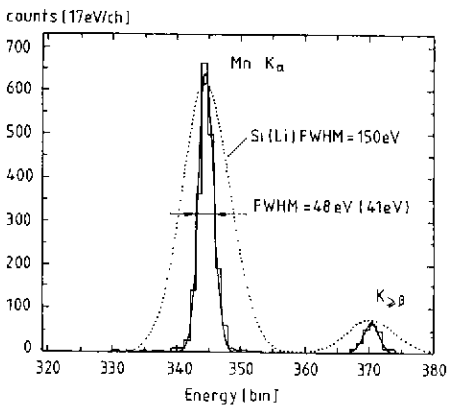

Fig. 15: Energy spectra from E $\simeq$ 6 keV γ rays obtained at PSI using a Sn STJ at T $\simeq$ 400 mK. Shown is, for comparison (dotted line), the best performance of a Si:Li semiconductor detector at LN_2 temperature.

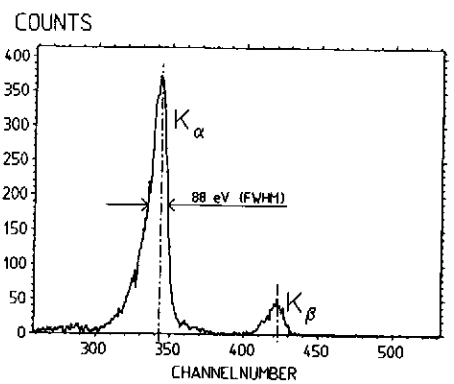

Fig. 16: Energy spectra for E $\simeq$ 6 KeV Mn γ rays obtained by the TMU (Garching) group using a Sn STJ at T $\simeq$ 400 mK.

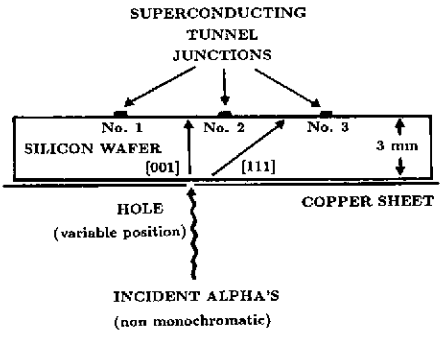

Fig. 17 a): Rough scheme of a set-up for ballistic phonon studies, based on work by the TMU (Garching) group. From the impact point selected through the hole position, phonons propagate following the main crystallographic axis and are collected by the STJ read-out implanted on the opposite side of the silicon wafer.

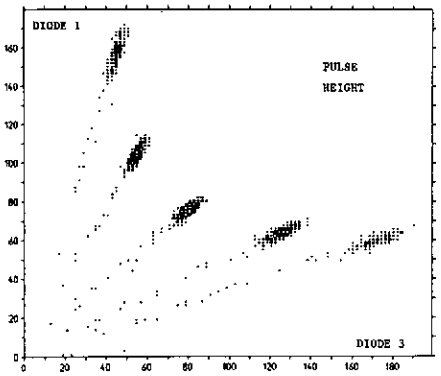

Fig. 17 b): Two-junction pulse height scatter plot, for several positions of the incident α particles on the lower face of the Si wafer. Correlations providing position information are clearly exhibited. Reported by F. von Feilitzsch et al. at the Bugey Workshop on Reactor Neutrino Physics, Sept. 88. The non-monochromatic spectrum of the ^{241}Am source used must be considered when evaluating energy resolution.

5. SUPERHEATED SUPERCONDUCTING GRANULES

A type I superconductor with low enough κ (the Ginzburg-Landau parameter) can exhibit metastable states (Fig. 18), due to the positive normal-superconducting interface energy. Type I samples may remain in the superconducting state for values of the external magnetic field larger than the critical field H_c (superheating). The superheated state has been obtained for pure metal microspheres of 1-400 μm diameter (Fig. 19). SSG detectors are usually prepared as a colloid of granules into some dielectric material, with read-out loops oriented in the plane normal to the applied magnetic field $\vec{H}_0$. The phase transition of one or several grains is thus detected through the disappearance of the Meissner effect. The flux variation produce a small current in the loop. Shape inhomogeneities, surface defects, as well as diamagnetic interactions, lead to a broad differential superheating curve is observed (Fig. 20), where dN/dH_0 is the number of granules changing state per unit increase of the applied magnetic field H_0.

It was proposed long ago [58] to use SSG as a particle detector. The energy released by an incident particle, when converted into heat, would originate a fast transition of the grains where the interaction took place. Recently, progress has been made in the SSG real time read-out [59] and granules of sizes 10-400 μm have been shown to be sensitive to low energy sources down to 6 keV γ's [60]. The observed sensitivity (Fig. 21, 22) can be theoretically understood and, when extrapolated to very small grains, gives encouraging figures: 1 μm diameter In grains at T = 200 mK would be sensitive to about 300 eV with 80% efficiency, whereas Ga grains cooled to 100 mK would achieve a similar performance for 4 eV energy deposition. Unfortunately, even if these figures could be obtained in a realistic detection system, two types of experiments would still remain quite difficult:

1) It has been proposed [11] to use indium SSG as a detector for low energy solar neutrinos, exploiting the SSG potentiality in segmentation (crucial for background rejection). A X-Y current loop read-out (Fig. 23) would allow to segment a 4 ton indium detector into 10^7 elementary cells, with only 10^5 electronic channels. However, such an instrumentation would require 5 mm × 1 m current loops, which makes extremely difficult to detect the signal produced by 116 keV secondaries.

2) Dark matter searches through nucleus recoil encounter an even more severe difficulty, since only single grain flips are usually expected. The device is seen as a threshold detector, without any energy resolution.

To cure both diseases, we have proposed a new operating principle, based on the concept of "amplification by thermal micro-avalanche" [12, 19]. Metastability allows for a positive latent heat in the superconducting to normal phase transition, due to the fact that an external magnetic field higher than H_c is involved in the process. The extra magnetic free energy stocked in superheating may then be large enough to change the thermal nature of the transition, which is endothermic at equilibrium.

In such case, the flip of a single granule will release heat which, together with the deposited energy, will be dispersed in the detector. If heat exchanges through the dielectric material are efficient enough (low Kapitza resistances), new flips will be produced which in turn release more latent heat. In such a scenario, with sufficiently small grains (1 μm in diameter), a signal in magnetic flux $\Delta\Phi \propto E$ is expected even for a nucleus recoil. The appearance of extra flips will lead to an amplification effect (one or two orders of magnitude), which may solve the basic problems for a ^{115}In experiment. Time resolution is expected to be in the range 10-100 ns, for good heat diffusion and low Kapitza resistances.

Other applications would then be possible: double beta decays [61], X-ray imaging [62], dark matter searches through inelastic scattering with a ^{119}Sn target [19]. Furthermore, the dielectric material can provide an active target (hydrogen for dark matter searches [19])... However, if experimental evidence for global avalanches already exists [63], further work is required to evaluate the real performance of the micro-avalanche effect. Another crucial problem is large scale production of very small grains. ϕ_{mean} (average size) $\simeq$ 25 μm tin granules are produced [64] at a rate of 5 kg/hour using a 40 kHz ultrasonic atomizer. A new development is underway in order to adapt the existing procedure to higher ultrasonic frequencies, up to 5 MHz according to the law [65]: $\phi_{mean} \propto f^{-2/3}$.

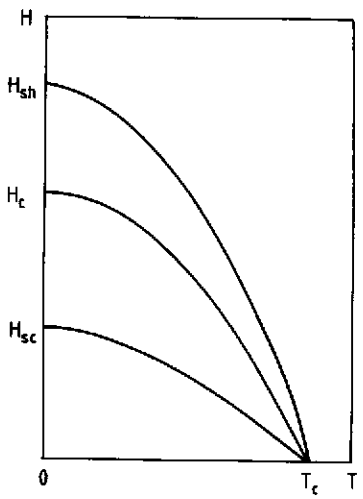

Fig. 18: Phase diagram of a type I superconductor incorporating metastable states. H_{sh} and H_{sc} are respectively the superheated and supercooled critical field.

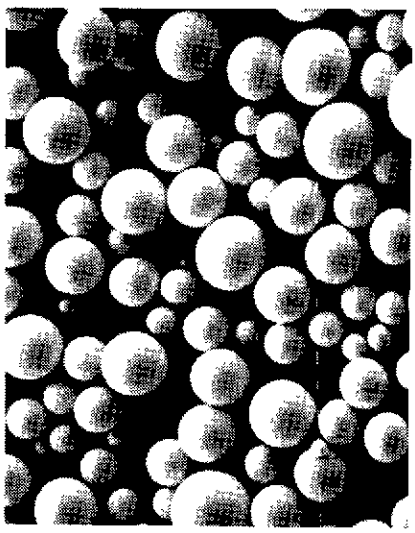

Fig. 19: Tin granules recently produced by EXTRAMET [64]. The mark is 10 μm.

An independent application, using large grains, would be the detection of magnetic monopoles [24], where the flux tube injected by the monopole would destroy the superconductivity of many granules. The advantage of SSG would be a comfortable signal (several orders of magnitude larger than in induction experiments), a good background rejection due to the large grain size, and a measurement of speed and direction.

6. MICRO-KELVIN DEVICES

Nuclear cooling techniques [66] have been recently improved down to 10-20 μK. Studies of superfluid ^{3}He are performed down to 100 μK.

When a magnetic field is applied to a nuclear spin system, a level splitting is produced and the new levels are populated in a temperature-dependent way. If the applied field is increased isothermally, and the sample is then thermally decoupled from the outside world, a microkelvin device has been potentially created. Due to the very high specific heat of the nuclear spin system at very low temperature, most of internal energy has been stocked in the form of spin excitations. Lowering again the

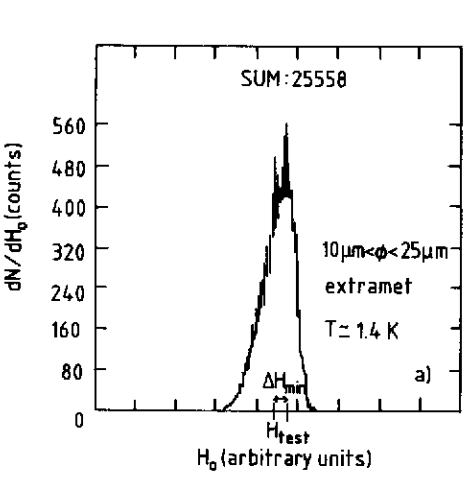

Fig. 20: A typical differential superheating curve for a tin SSG colloid. dN/dH_0 is the number of granules changing state per unit increase in applied magnetic field H_0.

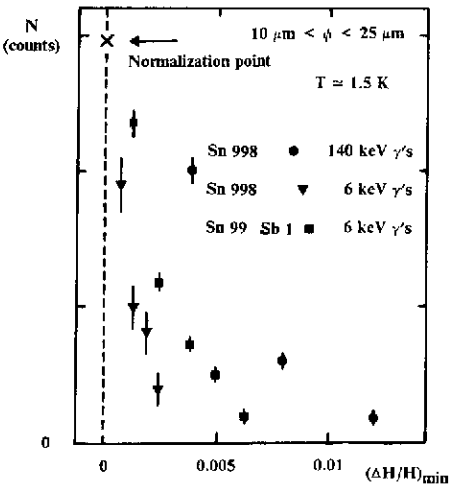

Fig. 21: Irradiation results for several tin SSG samples at ^{4}He temperature. N is the number of flips after a certain time, and $(\Delta H/H)_{min}$ stands for a small sweep in H_0 setting an equivalent energy threshold. From the authors, in [33].

magnetic field, level splitting is removed taking away most of the internal energy of the sample. The nuclear spin system, cooled by demagnetization, pumps in turn energy from the electron gas from contact spin-flip interactions (spin-lattice relaxation). The heat absorption rate by the nuclear degrees of freedom is governed by the equation [66]:

$$dQ/dt = n\,A\,B^2\,\tau^{-1}\,(T_n^{-1} - T_e^{-1}) \qquad (11)$$

where n is the molar density, A the Curie constant, τ the spin-lattice relaxation time, T_n the nuclear temperature and T_e the electronic temperature. A commonly used material is copper, which has a reasonably short spin-lattice relaxation time: $\tau \approx 1\ s\ (T/K)^{-1}$, and a moderately high Curie constant: $A = 3.188\ 10^{-6}\ J\ K\ T^{-2}\ mol^{-1}$. In this way, extremely low temperatures (down to 13 μK) are produced. Ultra-low temperature machines based on this principle exist in several laboratories: Julich [67], Tokyo [68], Helsinki [69], Bayreuth [70], and Lancaster [71].

Although it is too early to evaluate the relevance of such devices for practical detection purposes, the opening of a new technological window to the study of very low energy deposition must be acknowledged. Even in their present form, sub-millikelvin machines have been considered as a way to study galactic dark matter [72]. The basic idea is to use residual heat leaks to get bounds on two processes: i) single nucleus coherent scattering, where energy is transmitted as a single nucleus recoil [53]; ii) coherent 1-phonon scattering (involving several nuclei), which occurs for λ (wavelength) much larger than the basis vectors of the lattice structure. According to [72], process i) dominates for m (particle mass) > 20 MeV, whereas process ii) manifests itself for m < 20 MeV. Unfortunately, the obtained bounds are far away from realistic goals in the second region, which would be relevant to the detection of cosmological neutrinos.

The use of superfluid ^{3}He as a particle detector at $T \simeq 100\ \mu K$ has equally been considered [73], where a 1 eV energy deposition would excite $\approx 10^7$ quasiparticles. These quasiparticles consist of ^{3}He atoms and are therefore electrically neutral. No physical principle has been foreseen to build a realistic read-out for such excitations.

7. OTHER DEVICES

Energy deposited in superfluid ^{4}He at low temperature (100 mK) would create rotons ($\Delta/k = 8.65$ K). A 200 keV electron from neutrino scattering is expected to originate $\approx 10^8$ elementary excitations, which will propagate ballistically in all directions. Some will hit the surface of the liquid and evaporate a sizeable number of helium atoms, that may be detected by bolometric techniques [74]. No experimental result exists yet on this technique, but a development is being carried on at Brown University.

If cryogenics can be successfully incorporated in high energy experiments, superconductive devices present potentially the advantage of an excellent radiation hardness, due to the stability of superconducting parameters with respect to defects, as compared to solid scintillators and semiconductors. Thus, superconductors could be used as micro-vertex and very forward tagging detectors. CERMET devices [75], made of NbN films operating as flux flow detectors at 6 K, or superconducting β-Ga granules ($T_c = 5.9$ K) may be interesting possibilities. A vertex detector is being developed [76], based on the propagation of the hot spot created by and incident particle in a superconducting strip or wire biased by a current $I < I_c$. Current dissipation provides extra energy, at a power per unit volume $W_I = \rho\ J^2$, where J is the current density and ρ the normal state resistivity. The thermal energy absorbed by the medium is in turn: $W_M \simeq c^2\ \Delta T\ \kappa^{-1}$. If $W_J > W_M$, the hot spot propagates along the two directions of the one-dimensional sample and may lead to a high-resolution position detector. Hot spot propagation speed is $\approx 10^3$ m/s.

A successful application of cryogenic techniques is the use of low temperature electromagnetic cavities for the detection of galactic axions. In this case, low temperature ($T = 4.2$ K) is used to lower the resistance of a copper cavity and improve the quality factor $Q = (\omega_o\ R\ C)^{-1}$, where ω_o is the resonant frequency, and R, C the equivalent series resistance and capacity. It also allows for the use of a cold GaAs narrow band amplification stage. Superconducting materials are avoided, for they would lead to unwanted persistent currents. Due to the $a\gamma\gamma$ coupling [4, 16], a galactic axion can turn into a photon in the presence of an intense electromagnetic field. Since galactic halo particles are expected to be non-relativistic ($v \sim 10^{-3}$ c), $a \rightarrow \gamma$ conversion would produce a narrow line, of energy $E \simeq m_a$, and width $\Delta E/E \approx 10^{-6}$. In a low noise cavity, with an applied magnetic field B as large as possible, axion conversion would produce an electromagnetic signal of frequency $\nu = E/h \simeq m_a/h$. The resonant frequency of the cavity can be tuned with the help of a sapphire rod (Fig. 24), allowing to explore a wider frequency range by successive scans. In this way, an active search is being carried out in the $f \approx 1$ GHz range, which corresponds to the value of the axion mass ($m \approx 10^{-5}$ eV) for which this particle may close the universe.

Present cosmic axions detectors have already been able [17] to put bounds only a factor of 50 below cosmological flux predictions [77, 4]. Such a far-reaching effort should certainly be pursued in order to check cosmological limits.

Finally, the use of induction loops for magnetic monopole detection is by now a running program where considerable technological skill has been developed. In the presence of magnetic charges, Faraday's law becomes:

$$\vec{\nabla} \times \vec{E} + 1/c\ \partial\vec{B}/\partial t = 4\pi/c\ \vec{j}_m \qquad (12)$$

where $\vec{j}_m$ is the magnetic current density. A magnetic charge n (in Dirac units [78]), when passing through a superconducting loop of inductance L, will induce a dc current $i = 2n\Phi_o/L$, where Φ_o is the flux quantum, $\Phi_o = hc/2e \simeq 2 \times 10^{-7}$ Gauss cm^2. This current is rather small ($i \simeq 2$ nA for $L = 1\ \mu$H), but can be read by a SQUID (chapter 8, sect. 2). The main problem, in such experiments, is noise background coming from external electromagnetic signals (including earth's magnetic field fluctuations $\approx 10^{-3}$ gauss). To escape such backgrounds, gradiometric loops have been designed. Furthermore, superconducting lead can provide an active shield [21, 23], where the monopole will inject a flux tube $\Phi = 2n\ \Phi_o$, that can be detected by a scanning procedure. μ-metal is another possible shielding, although less powerful than lead. In such case, the gradiometric technique is pushed to its highest performance (e.g. Fig. 25) and coincidences are used [79, 80].

Induction loops have brought two well-known candidate events, which are not well established nor have been confirmed by subsequent runs. In spite of the high degree of noise rejection reached by prototypes of several m^2, background problems are likely to grow with detector surface, due to the smallness of signals involved. It remains that no other detection technique is known allowing to: a) detect monopoles of any speed through an interaction derived directly from first principles; b) directly measure the monopole magnetic charge. This motivation appears strong enough to pursue the induction program in spite of all technical difficulties.

Non-superconducting induction devices producing transient responses are also being considered [81], and ~ 10 cm loops operating at LN_2 temperature have been built. High T_c superconductors may also be an interesting alternative, especially since the feasibility of YBaCuO SQUIDs has been demonstrated [82].

8. LOW TEMPERATURE ELECTRONICS

8.1 Conventional

The main motivations for the use of conventional electronics at cryogenic temperatures are the lower noise produced by random motion of current carriers (thermal noise), the increase of the transconductance, the lower power dissipation and signal distortion through transmission lines, the larger carrier

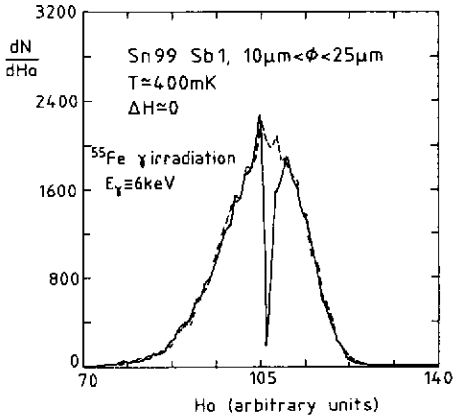

Fig. 22: Irradiation result for a $Sn_{99}Sb_1$ SSG sample at ^{3}He temperature. The granules missing in the irradiated differential superheating curve (full line), as compared to the non-irradiated one (dashed line), are those having changed state during an irradiation at $\Delta H_{min} = 0$, and were counted in real time during this period. From the authors, in [33].

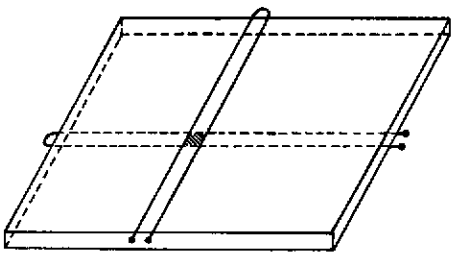

Fig. 23: A typical read-out principle for SSG detectors. Long current loops (read by conventional electronics) are deposited in X- and Y-planes between foils of SSG colloid. X-Y coincidence between two loops provides then position information with excellent accuracy.

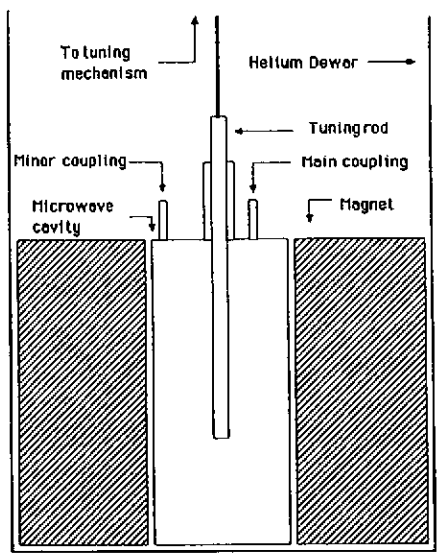

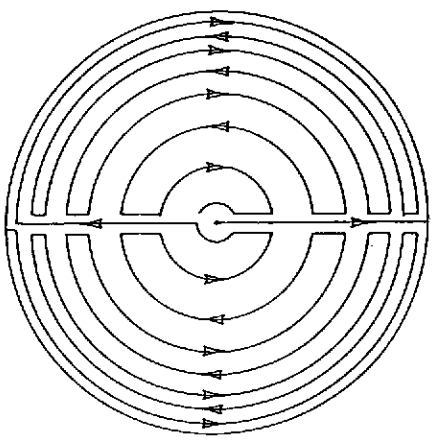

Fig. 25 (above): Basic design of a gradiometric low background induction loop for monopole detection. From [81].

Fig. 24 (left): Basic design of the cryogenic copper cavity BNL-Rochester-FNAL cosmic axion detector, from [17].

mobility leading to faster operating speed at a given capacitance, and the possible use of low gap, high mobility materials. The exponential fall of leakage currents is a crucial advantage when dealing with highly sensitive charge amplifiers.

However, decreasing the temperature leads to a reduction of the carrier population and, in the case of undoped silicium, to a complete "freeze-out" of the carrier at T ≈ 4 K. Doping impurities lower the energy gap and improve low T carrier density, but increase in turn the number of trapping centers.

Thermal (Johnson) noise is the dominant component of electronic noise at high frequency, and

falls significantly at low T, according to the law:

$$e^2 = 4\,KT\gamma/g_m \tag{13}$$

where g_m is the transconductance (Gain $= g_m R_L$, R_L is the load resistance) and $\gamma = 0.5$-0.6. Below some device-dependent frequency band, generation-recombination rate fluctuations provide the dominant (1/f) component (flicker noise), which, usually, decrease strongly with T. Fig. 26 shows the T-dependence of noise at all frequencies for a Ge FET and a GaAs FET. The low temperature behavior of several semiconductors is well described in Fig. 27, which shows the temperature dependence of conductivity for several materials. Si conductivity drops dramatically below 100 K, whereas n-InSb shows the best performance, with remarkable stability down to ^{4}He temperatures. n-GaAs also shows good behavior at low T. The increase in electron mobility for low doping level semiconductors leads to an increase in JFET transconductance [83]. Fig. 28 shows the T-dependence of g_m for several commercially available devices, where scattering by ionized impurities appears to be of little significance down to T = 4 K.

Among the three main semiconductors families: silicon, germanium and Ga-As devices, only the last two remain operative at liquid He temperature (bipolar Si junction are even not usable at LN_2 temperature). The best overall signal over noise ratio for Si is obtained with JFET and MOSFET at 120 K. The following table shows some of the best results obtained so far [83, 84]. Going down from 4.2 K to 1.8 has not shown substantial variations.

Device	Noise nV/$\sqrt{\text{Hz}}$	Transconductance mA/V	Frequency range MHz	Temperature K
Si-JFET	0.75	20.	0.03-50	77
Si-MOSFET	1.0	40.	≈ 1	77
Ge-FET	1.2	13.	0.1-1	4.2
Ga-As-FET	3.0	38.	≈ 1	77
"	0.55	"	≈ 10	"

8.2 Superconducting

B. Josephson [85] showed that Cooper pair tunneling across a superconductor-insulator-superconductor (SIS) junction in the presence of an applied dc voltage V has the form: $I = I_c \sin\phi$, where I_c is called the critical current and depends on T and junction structure. ϕ is the phase difference between the phase of the Cooper pair wave function on both sides of the junction,

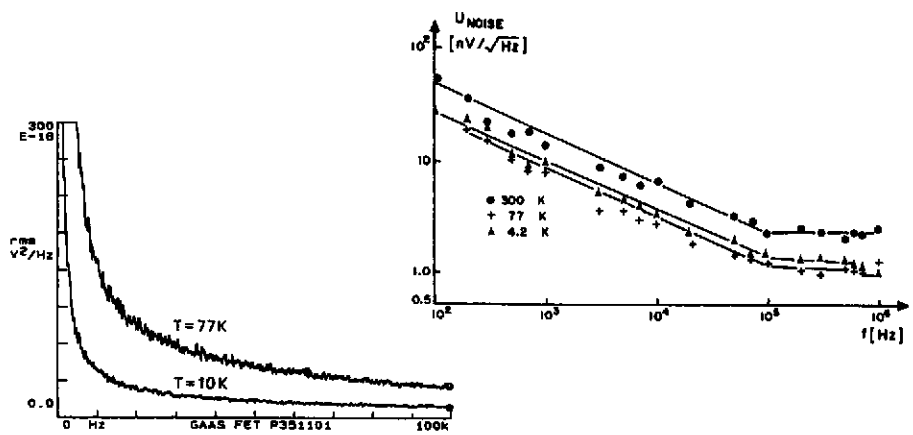

Fig. 26: Noise figure at several temperatures for a GaAs FET (left) from D. Camin et al. in [31], and for a germanium FET (right) from [83].

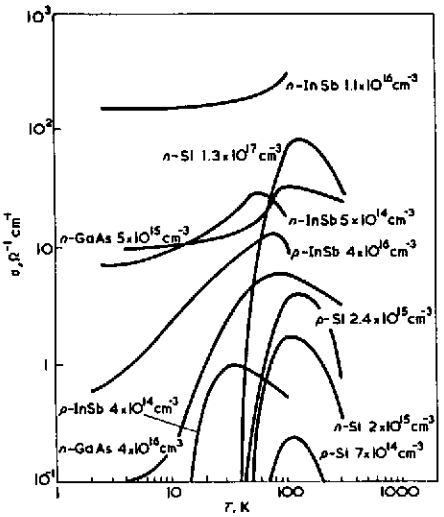

Fig. 27: T-dependence of conductivity for several semiconductor materials. From: B. Lengeler, Cryogenics 14, 439 (1974).

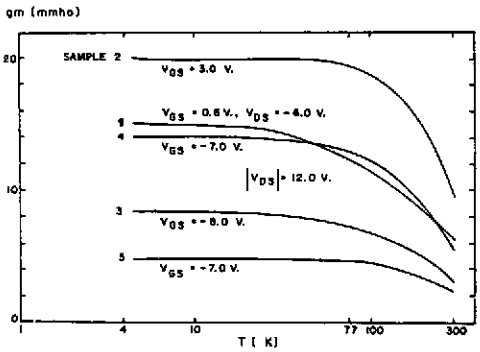

Fig. 28: T-dependence of transconductance for several commercially available FET, from [83]: 1) germanium TIX M12, channel p, operated in depletion mode; 2) silicon 2N 3797, n, depletion and enhancement; 3) Si 3N 160, p, enhancement; 4) Si MEM 517, p, enhancement; 4) Si MEM 520, p, enhancement.

and follows the law: $d\phi/dt = 2\ eV/\hbar$ leading to an ac current of frequency $f_j = eV/\pi\hbar$. In a real circuit, the relevant equation is [86]:

$$I = I_c \sin\phi + G\,V + C\,dV/dt \qquad \{14\}$$

where C is a capacitance representing the displacement current at the junction, and G a conductance accounting for quasiparticle tunneling and insulator leakage currents. Solving this equation, it is possible to obtain a characteristics of $<I>$ in terms of $<V>$. In the presence of an applied magnetic field, the characteristics is distorted through the relation:

$$I_c(\Phi) = I_c(0)\,|\,\sin(\pi\Phi/\Phi_0)\,/\,(\pi\Phi/\Phi_0)\,| \qquad \{15\}$$

where Φ is the magnetic flux through the junction and Φ_0 the flux quantum. This distortion is the basic principle for the detection of RF signals in 1-junction detectors (RF SQUID).

More recently, dc SQUID have been developed based on a two-junction parallel array. In this case, a magnetic field perpendicular to the plane of the array causes a difference in the values of phase shifts through the two junctions. If ϕ_1 and ϕ_2 are the phase differences in junctions 1 and 2 taken in the same (parallel) direction, one has: $\phi_1 - \phi_2 = 2\pi\ \Phi/\Phi_0$, where Φ is now the flux through the surface surrounded by the circuit. If both junctions have the same I_c, the maximum total current through the parallel array becomes:

$$I_{T,C} = 2\,I_c\,|\cos\pi\Phi/\Phi_0\,| \qquad \{16\}$$

The intensity modulation caused by the applied magnetic flux results in a modulation of the voltage across the SQUID. The equivalent flux noise of a dc SQUID can be made as low as [87]:

$$\varepsilon/1\text{Hz} \approx 16\ kT\ (LC)^{1/2} \qquad \{17\}$$

where ε is an energy equivalent to the magnetic flux noise $\delta\Phi$: $\varepsilon = (\delta\Phi)^2/L$ and L the loop inductance. It must be noticed, however, that: a) 1/f noise appears at $f < 10$ Hz ; b) at $T < 1$ K, the noise of the conventional amplifier following the SQUID is likely to become dominant.

Superconducting electronic devices are not substitutes of conventional semiconductor amplifiers. They are mainly very low noise, highly sensitive, low impedance detectors of electromagnetic signals. A stage of conventional electronics is then coupled to the SQUID output and eventually provides the high gain of the read-out. The appearance of high T_c superconductors opens the way to the design of very interesting hybrid devices [88], where superconducting junctions and semiconductor components may be integrated in a single chip, working at some temperature in the range 4 K-100 K.

9. CONCLUSION

Cryogenic devices for particle detection are being developed in many laboratories, all over the world, as physics motivation is becoming more and more obvious and widespread. Recent progress on the basic understanding of cryogenic detectors is rather impressive, and particle irradiation results are encouraging. In the last two years, these developments has been successfully integrated into a new cross-disciplinary field, at the frontier between particle physics, astronomy and materials science. However, many new ideas remain to be tested, and important improvements are still necessary to evolve from workbench prototypes to real detectors.

In the meantime, some cryogenic detectors (induction loops for monopoles, electromagnetic cavities for cosmic axions, gravitational antennas,...) are being successfully operated by particle physicists and already demonstrate basic advantages of low temperature, such as low noise and high sensitivity.

References

[1] See, for instance, "'86 Massive Neutrinos in Astrophysics and in Particle Physics", Ed. O. Fackler and J. Tran Thanh Van, Frontières 1986.

[2] See, for instance, "New and Exotic Phenomena", Ed. O. Fackler and J. Tran Thanh Van, Frontières 1987.

[3] See, for instance, "5^{th} Force - Neutrino Physics", Ed. O. Fackler and J. Tran Thanh Van, Frontières 1988.

[4] See, for instance, R. Peccei in [2] and references therein.

[5] See, for instance, "Dark Matter", Ed. J. Audouze, Frontières 1988.

[6] See, for instance, G. Gelmini, ISAS preprint 111/87/EP.

[7] See, for instance, G. Giacomelli, Riv. Nuovo Cimento 7, 1 (1984).

[8] N. Coron et al., Nature 314, 75 (1985).

[9] F. Cardone and F. Celani in [33].

[10] A. Drukier and L. Stodolsky, Phys. Rev. D30, 2295 (1984).

[11] Rapport de la Jeune Equipe "Neutrino-Indium" du CNRS (ENS Paris, LPC College de France, Ecole Polytechnique, DPhPE Saclay, IP Strasbourg, LAPP Annecy), January 1987.

[12] L. Gonzalez-Mestres and D. Perret-Gallix in [2].

[13] See, for instance, N. Booth et al. in [31].

[14] E. Fiorini in [31].

[15] M. Buhler and E. Umlauf, Europhys. Lett. 5, 297 (1988)

[16] P. Sikivie, Phys. Rev. Lett. 51, 1415 (1983).

[17] S. de Panfilis et al. in [33].

[18] A.K. Drukier, K. Freese and D. Spergel, Phys. Rev. D33, 3495 (1986).

[19] L. Gonzalez-Mestres and D. Perret-Gallix, in [5].

[20] B. Cabrera, F. Wilczeck and L. Krauss, Phys. Rev. Lett. 55, 25 (1985).

[21] See, for instance, B. Cabrera in [32].

[22] Th. Peterreins, F. Probst, F. von Feilitzsch, and H. Kraus, in [32].

[23] D. Caplin in [2].

[24] L. Gonzalez-Mestres and D. Perret-Gallix, Proceedings of Underground Physics 85, Ed. Il Nuovo Cimento (1986).

[25] C. Chaillout in [33].

[26] See, for instance, "Superconductivity", Ed. R. D. Parks, M. Dekker Inc. 1969.

[27] See, for instance, N.W. Ashcroft and N.D. Mermin, "Solid State Physics", Ed. Holt, Rinehart & Winston 1976.

[28] P.D. Thatcher, Phys. Rev. 156, 975 (1967).

[29] J.J. Chang and D.J. Scalapino, J. Low Temp. Phys. 31, 1 (1978).
C.C. Chi, M.M.T. Loy and D.C. Cronemeyer, Phys. Rev. b23, 124 (1981).

[30] J. Lindhard et al. Kgl. Dan. Vidensk., Selsk., Mat. Fys. Medd., 33, 10 and 14 (1963).

[31] "Low Temperature Detectors for Neutrinos and Dark Matter", Ed. K. Pretzl, N. Schmitz and L. Stodolsky, Springer-Verlag 1987.

[32] "Superconductive Particle Detectors", Ed. A. Barone, World Scientific Pub. 1987.

[33] "Low Temperature Detectors for Neutrinos and Dark Matter-II", Ed. L. Gonzalez-Mestres and D. Perret-Gallix, Frontières 1988.

[34] D. Curie, "Luminescence in Crystals", Methuen & Co. 1963.

[35] G. Boulon, Revue Phys. Appl. 21, 689 (1986).

[36] M.J. Treadaway and R.C. Powell, Journal Chem. Phys. 61, 4003 (1974).

[37] R. Moncorge, Thesis Lyon 1976.

[38] F. Rogemond, Thesis Lyon 1986.

[39] B. Jacquier, in [33] and private communication.

[40] J. Mares, Czech. J. Phys. B35, 883 (1985).
[41] M.J. Weber, J. Appl. Phys. 44, 3205 (1973).
[42] J. Mares, B. Jacquier, C. Pedrini and G. Boulon, Revue Phys. Appl. 22, 145 (1987).
[43] K. Takagi and T. Fukazawa, Appl. Phys. Lett. 42, 43 (1983).
[44] S.M. Sze, "Physics of Semiconductor Devices", John Wiley & Sons 1981.
[45] U. Fano, Phys. Rev. 70, 44 (1946); 72, 26 (1947).
[46] D.O. Caldwell in [2].
[47] See, for instance, "Semiconductors and Semimetals", Vol. 12 "Infrared Detectors II", Ed. R. K. Willardson and A.C. Bear, Academic Press 1977.
[48] See, for instance, E.E. Haller and F.S. Goulding, in "Handbook of Semiconductors", Vol. 4, Ed. C. Hilsum, North-Holland 1981.
[49] S.H. Moseley, J.C. Mather and D. Mc Cammon, J. Appl. Phys. 56, 1257 (1984).
[50] D. Mc Cammon et al., Proc. 18th Conference on Low Temp. Phys., Kyoto 1987; Jap. J. Appl. Phys. 26, Suppl. 26-3.
[51] A. Alessandrello, D.V. Camin, E. Fiorini and A. Giuliani, Phys. Lett. 202, 611 (1988).
[52] H.H. Stroke et al., IEEE Trans. on Nucl. Sc. 33, 56 (1986).
[53] M.W. Goodman and E. Witten, Phys. Rev. D31, 3059 (1985).
[54] D. Twerenbold and W. Rothmund, A. Zehnder in [32].
[55] Th. Peterreins, F. Probst, F. von Feilitzsch and H. Kraus, in [32].
[56] P. Gare et al., ESA preprint (1988).
[57] R.S. Raghavan, Phys. Rev. Lett. 37, 259 (1976).
[58] H. Bernas et al., Phys. Lett. 37, 359 (1967).
[59] A. Kotlicki et al. in [31]; A. de Bellefon et al. in [33]; J. Boniface et al., in [33].
[60] For a review of recent results and possible uses, see: L. Gonzalez-Mestres and D. Perret-Gallix, in "Superconductive Particle Detectors" and in ref. [3]; K. Pretzl, same references.
[61] P. Andreo, J. Garcia-Esteve and A.F. Pacheco, in ref [31].
[62] C. Valette, G. Waysand, Orsay report (1976).
[63] F. von Feilitzsch et al. in [31].
[64] EXTRAMET, Zone Industrielle, Annemasse (Haute-Savoie), France.
[65] E.G. Lierke and G. Grießhammer, Ultrasonics October 1967, p. 224.
[66] See, for instance, G. Pickett, Rep. Prog. Phys. 51, 1295 (1988).
[67] R.M. Mueller et al., Cryogenics 20, 395 (1980).
[68] H. Ishimoto et al., J. Low Temp. Phys. 55, 17 (1984).
[69] M. Huiku et al. J. Low Temp. Phys. 62, 433 (1986).
[70] P. Smeibdl et al., Japan. J. Appl. Phys. 26, Suppl. 26-3, 1715 (1987).
[71] D.I. Bradley et al., Cryogenics 22, 296 (1982).
[72] T.O. Niinikoski, in Proc. "Rencontre sur la Masse Cachée dans l'Univers et la Matière Noire", Annecy July 8-10 1987, Ed. Annales de Physique (France), and in preparation.
[73] G.R. Pickett, in [33].
[74] R. Lanou, H. J. Maris and G. Seidel, in ref. [31].
[75] S. King and G.G. Fritz in [33]
[76] O. Liengme in [31] and in [32]; R.G. Wagner and K.E. Gray in [32].
[77] M. Dine, W. Fischler and M. Schrednicki, Phys. Lett. 104B, 199 (1981).
[78] P.A.M. Dirac, Proc. Royal Soc. London A133, 60 (1931).
[79] S. Bermon et al., Phys. Rev. Lett. 53, 2067 (1984).
[80] S. Somalwar, H. Frisch, J. Incandela and M. Kuchnir, Nucl. Inst. Meth. A226, 341 (1984).
[81] See, for instance, J. Incandela, in ref. [3].
[82] D. Robbes in [33].
[83] S.S. Sesnic and G.R. Craig, IEEE Trans. Electron. Devices, ED-19, 933 (1972).
[84] F.Celani, V. Gambardella, A. Giorgi, A. Sagesse, J. Cata and S. Pace in "Low Temperature Electronics and High Temperature Superconductors", Ed. S.I. Raider, R. Kirschman, H. Hayakawa and H. Ohta, The Electrochemical Society, Inc.
[85] B. Josephson, Phys. Lett. 1, 251 (1962).
[86] See, for instance, T. van Duzer and C.W. Turner, "Principles of Superconducting Devices and Circuits", Ed. Elsevier North Holland, New York 1969.
[87] See, for instance, J. Clarke in Proc. XVII Int. Conf. on Low Temp. Phys., Karlsruhe 1984.
[88] T. van Duzer, Cryogenics 28, 527 (1988).